Appl. Chem. Eng., Vol. 34, No. 5, October 2023, 548-555
https://doi.org/10.14478/ace.2023.1072

Article

Conversion of Dimethyl Ether to Light Olefins over a Lead-Incorporated SAPO-34 Catalyst with Hierarchical Structure

Kang Song, Jeong Hyeon Lim, Young Chan Yoon, Chu Sik Park* and Young Ho Kim†

Department of Chemical Engineering and Applied Chemistry, Chungnam National University, Daejeon 34134, Republic of Korea
**Korea Institute of Energy Research, Daejeon 34129, Republic of Korea*
(Received August 18, 2023; Revised September 3, 2023; Accepted September 4, 2023)

Abstract

SAPO-34 catalysts were modified with polyethylene glycol (PEG) and Pb to improve their catalytic lifetime and selectivity for light olefins in the conversion of dimethyl ether to olefins (DTO). Hierarchical SAPO-34 catalysts and PbAPSO-34 catalysts were synthesized according to changes in the molecular weight of PEG (M.W. = 1000, 2000, 4000) and the molar ratio of Pb/Al (Pb/Al = 0.0015, 0.0025, 0.0035), respectively. By introducing PEG into the SAPO-34 catalyst crystals, an enhanced volume of mesopores and reduced acidity were observed, resulting in improved catalytic performance. Pb was successfully substituted into the SAPO-34 catalyst frameworks, and an increased BET surface area and concentration of acid sites in the PbAPSO-34 catalysts were observed. In particular, the concentrations of the weak acid sites, which induce a mild reaction, were increased compared with the concentrations of strong acid sites. Then, the P2000-Pb(25)APSO-34 catalyst was prepared by simultaneously utilizing the synthesis conditions for the P2000 SAPO-34 and Pb(25)APSO-34 catalysts. The P2000-Pb(25)APSO-34 catalyst showed the best catalytic lifetime (183 min based on DME conversion > 90%), with an approximately 62% improvement compared to that of the unmodified catalyst (113 min).

Keywords: *Dimethyl ether to olefins, SAPO-34, Pb Substitution, Polyethylene glycol, Mesopores*

1. Introduction

Light olefins (ethylene, propylene) are important basic raw materials in the petrochemical industry, and the demand for light olefins is rapidly increasing[1]. Light olefins are mainly produced through the naphtha cracking process with petroleum. However, due to increasingly stringent environmental regulations and because the supply and demand of petroleum is instable, the methods for producing light olefins from nonpetroleum materials have attracted attention from many researchers[2-6]. The methanol to olefins (MTO) or dimethyl ether to olefins (DTO) process is a process of producing light olefin using methanol or dimethyl ether (DME) as raw materials. This process produces lower carbon dioxide (CO_2) emissions than that of the naphtha cracking process[7,8]. In addition, methanol and DME, which are produced from natural gas, coal, and biomass, can replace the supply and demand instability of petroleum[9].

The SAPO-34 catalyst is a promising catalyst that exhibits high selectivity for light olefins in the MTO or DTO process. The SAPO-34 catalyst has a three-dimensional chabazite (CHA) structure and shows shape selectivity toward light olefins due to its small pore size (0.38 nm), and the catalyst is composed of an 8-membered ring[10]. It was reported that methanol or DME are converted to light olefins by a dual-cycle mechanism[11]. The reactants diffuse into the catalyst cage and are then converted to linear olefins (C_nH_{2n}) by a chain reaction (alkene cycle). The C_6H_{12} produced by the chain reaction is converted to hexamethyl benzene (HMB) through aromatization and by reacting with reactants (arene cycle). Light olefins are generated by the cracking of linear olefins (alkene cycle), and an additional reaction and cracking with HMB and reactants (arene cycle). However, as the reaction proceeds, polyaromatic hydrocarbons (PAHs), which are the cause of coke formation, are produced through the condensation and cyclization of HMB. The diffusion of reactants and products is limited by the cage being filled with coke. As a result, the SAPO-34 catalyst is rapidly deactivated, resulting in a short lifetime. Therefore, studies have been necessary to enhance the catalytic lifetime.

To improve catalytic performance, numerous studies have been conducted to modulate the acidity of catalysts and to enhance the mass transfer of reactants and products[12-20]. The acidity of the SAPO-34 catalyst can be controlled through adding isomorphous substitutions of various divalent metals (Co^{2+}, Ni^{2+}, Fe^{2+}, etc.) into the catalyst framework[12-14]. The acid sites of the SAPO-34 catalyst are created by forming Si-OH-P bonds through substituting Si^{4+} and P^{5+} into aluminophosphates (AlPOs) that are composed of an Al-O-P framework[12]. In addition, the P-OH-(nMe, (4-n)Al) framework can be formed by substituting Me^{2+} and Al^{3+}. The substitution of Me^{2+} influences the arrangement of Si atoms and, as a result, varies the catalyst acidity[13].

† Corresponding Author: Chungnam National University
Department of Chemical Engineering and Applied Chemistry, Daejeon 34134, Republic of Korea
Tel: +82-42-821-5898 e-mail: yh_kim@cnu.ac.kr

pISSN: 1225-0112 eISSN: 2288-4505

Kim et al. reported that the prepared CoAPSO-34 catalyst exhibited superior catalytic performance than that of SAPO-34 due to an increased concentration of weak acid sites[14]. Hierarchical SAPO-34 catalysts can be prepared by introducing various secondary templates as mesopore directing agents during the synthesis process[15]. The hierarchical structure of the SAPO-34 catalyst shows an improved mass transfer rate due to shorter reaction pathways. The formation of coke is suppressed by reactants and products with an enhanced mass transfer rate, which is a cause of catalyst deactivation, resulting in superior catalytic performance[16]. Schmidt et al. reported that a hierarchical SAPO-34 catalyst was prepared using carbon nanotubes (CNTs) as the secondary template[17]. Sun et al. reported that polyethylene glycol (PEG) was used to create a hierarchical structure, and the prepared hierarchical SAPO-34 catalyst showed superior catalytic performance in the MTO reaction[19]. Thus, the hierarchical structure improves the mass transfer of reactants and products, and the incorporation of metal adjusts the acidity distribution of the catalyst, resulting in enhanced catalytic performance. It is well known that PEG is used as a mesopore-directing agent due to its water solubility and ease of elimination during the calcination process[16]. Furthermore, Pb^{2+}-incorporated beta zeolite was successfully prepared by the dry impregnation method and showed superior catalytic performance in the aminolysis reaction of epoxides due to variations in acidity[21]. However, studies on the application of Pb^{2+} to hierarchical SAPO-34 catalysts have not yet been reported. Therefore, the performance of the hierarchical PbAPSO-34 catalyst must be confirmed in the DTO reaction.

In this study, the effects of adding PEG or Pb to the SAPO-34 catalyst were investigated to improve catalytic performance in the DTO reaction. First, the hierarchical SAPO-34 and Pb-incorporated SAPO-34 (PbAPSO-34) were prepared by adding the PEG molecular weight and Pb/Al molar ratio as variables, respectively. Afterward, the hierarchical PbAPSO-34 catalyst was prepared by simultaneously adding PEG and Pb. The physicochemical properties of the synthesized catalysts were analyzed by XRD, SEM–EDS, N_2 adsorption-desorption isotherms, XPS and NH_3-TPD. Moreover, the catalytic lifetime and selectivity of light olefins were evaluated by the DTO reaction.

2. Experimental

2.1. Materials

Aluminum isopropoxide (Junsei, 99%), LUDOX AS-40 (Sigma–Aldrich, 40%), and phosphoric acid (Samchun chemicals, 85%) were used as precursor materials for Al, Si, and P, respectively. Tetraethylammonium hydroxide (TEAOH, ACROS, 25%) and diethyl amine (DEA, Junsei, 99%) were used as structure directing agents (SDAs). Lead(II) nitrate ($Pb(NO_3)_2$, Samchun chemicals, 97%) was utilized as the metal source, and polyethylene glycol (PEG, molecular weight: 1000, 2000, 4000, Samchun chemicals, 99.5%) was used as the mesopore directing agent.

2.2. Preparation of catalysts

The SAPO-34 catalyst was prepared by a hydrothermal synthesis method. The molar composition for the synthesis of SAPO-34 catalysts was 1.0 Al_2O_3: 1.0 P_2O_5: 0.3 SiO_2: 1.0 TEAOH: 1.0 DEA: 52.0 H_2O (mol). Aluminum isopropoxide was added to a mixture of DEA and deionized water, and phosphoric acid was added dropwise while the mixture was stirred for 2 h (Sol A). Simultaneously, LUDOX AS-40 was added to TEAOH, and the mixture was stirred for 2 h (Sol B). The final gel was obtained by stirring the two mixtures for 2 h. For crystallization, the final gel was transferred to a Teflon-lined autoclave and heated at 200 °C for 72 h. After crystallization, the obtained solid product was washed, filtered, and dried at 60 °C for 12 h. Finally, the SAPO-34 catalyst was obtained by calcination at 600 °C for 6 h in an air atmosphere.

The hierarchical SAPO-34 catalyst was synthesized in the same molar ratio as for the abovementioned unmodified SAPO-34 catalyst except that 3.164 g of PEG (MW = 1000, 2000, 4000) was added to the gel, in which Sol A and Sol B were mixed before the crystallization step.

The synthesis procedure of the PbAPSO-34 catalyst was performed using the same method as the synthesis procedure of unmodified SAPO-34 except that metal salts of Pb/Al = 0.0015, 0.0025, and 0.0035 (mol) were added to the LUDOX-AS40 and TEAOH mixture (Sol B).

The hierarchical PbAPSO-34 catalyst was prepared by simultaneously adding PEG (M.W. = 2000) and Pb (Pb/Al = 0.0025). The catalyst preparation was performed by combining the synthesis procedure for the hierarchical SAPO-34 and PbAPSO-34 catalysts. The nomenclature of the prepared catalysts is shown in Table 1.

Table 1. The Nomenclature and Relative Crystallinity of the As-prepared SAPO-34 and Modified SAPO-34 Catalysts

Catalyst	Pb	PEG	Relative crystallinity (%)
	Molar ratio (Pb/Al)	Molecular weight	
SAPO-34	-	-	100
P1000 SAPO-34	-	1000	98
P2000 SAPO-34	-	2000	94
P4000 SAPO-34	-	4000	91
Pb(15)APSO-34	0.0015	-	112
Pb(25)APSO-34	0.0025	-	104
Pb(35)APSO-34	0.0035	-	86
P2000-Pb(25)APSO-34	0.0025	2000	94

2.3. Characterization of catalysts

The crystallinity of the prepared catalysts was characterized by X-ray diffraction (XRD, Rigaku Smartlab). The XRD measurements were performed using Cu Kα radiation in the angle range of $5° < 2\theta < 50°$ at voltages and currents of 45 kV and 200 mA. The morphology and size of the catalyst crystals were observed by scanning electron microscopy (SEM, S-4800, Hitachi). X-ray photoelectron spectroscopy (XPS, K-alpha+, Thermo) was conducted to investigate the chemical binding state of the catalyst surface. The Brunner-Emmett-

Teller (BET) surface area and pore structure of the catalysts were measured with N_2 adsorption-desorption isotherms, which were obtained using a Micrometrics Tristar Ⅱ. The acidity of the prepared catalysts was measured with NH_3-temperature programmed desorption (NH_3-TPD). The catalyst (0.2 g) was pretreated at 600 °C for 2 h with a He gas flow of 30 ml·min^{-1}. After pretreatment, NH_3 was injected into the catalyst at 100 °C for 1 h. Then, He gas was supplied to remove NH_3 that was physically adsorbed. Afterward, the chemically adsorbed NH_3 was desorbed under an He flow at temperatures from 100 °C to 700 °C. The desorbed NH_3 was analyzed through gas chromatography (GC, DS-6200, Donam) equipped with a thermal conductivity detector (TCD).

2.4. DTO reaction

The DTO reaction was carried out using a fixed bed reactor (O.D. = 1.1 cm) at 400 °C under atmospheric pressure. A total of 0.2 g of the catalyst (20-40 mesh) was loaded into the reactor. The process of pretreating the catalyst was conducted for 1 h at 400 °C under N_2 flow. After pretreatment, DME and N_2 were fed at a volume ratio of 1:3 using a mass flow meter (MFC). The weight hourly space velocity (WHSV) of DME was 3.54 h^{-1}. To remove the saturated hydrocarbons from the products, the water trap at 4 °C was equipped under the reactor. The reactant products were analyzed online with a gas chromatograph (GC, HP 5890 plus, Agilent) equipped with a capillary column (HP-plot Q, L 30 m × I.D. 0.320 mm) and a flame ionization detector (FID).

3. Result and discussion

3.1. Characterization of catalysts

The X-ray diffraction patterns of the prepared catalyst are shown in Figure 1. The unmodified SAPO-34 catalyst showed diffraction peaks corresponding to the CHA structure (2 θ = 9.5, 12.9, 16.1, 20.7, 30.9°)[15]. The catalysts modified with PEG or Pb exhibited the same diffraction peaks as the unmodified SAPO-34 catalyst, and no other diffraction peaks were observed. This means that the CHA structure was well formed in the modified SAPO-34 catalyst without variations in crystal structure or formations of amorphous phases[16]. This result indicates that Pb was successfully substituted into the framework of the SAPO-34 catalyst[22,23].

The relative crystallinity of the prepared catalysts was calculated by the sum of the intensities of the main peaks (2 θ = 9.5, 12.9, 20.76°) and is shown in Table 1[24]. Based on the crystallinity of the unmodified SAPO-34 catalyst being 100%, the relative crystallinity of the hierarchical SAPO-34 catalyst decreased as the molecular weight of PEG increased. This was attributed to the insertion of PEG into catalyst crystals, which caused crystal defects due to the mesopore formation that occurred during the calcination process[25]. The Pb(15)APSO-34 catalyst exhibited the highest relative crystallinity. However, as the amount of Pb added increased, a reduction in relative crystallinity was observed. It is suggested that the growth of the CHA structure is promoted by introducing Pb into the SAPO-34 catalyst framework but is inhibited as the amount of Pb added increases[26].

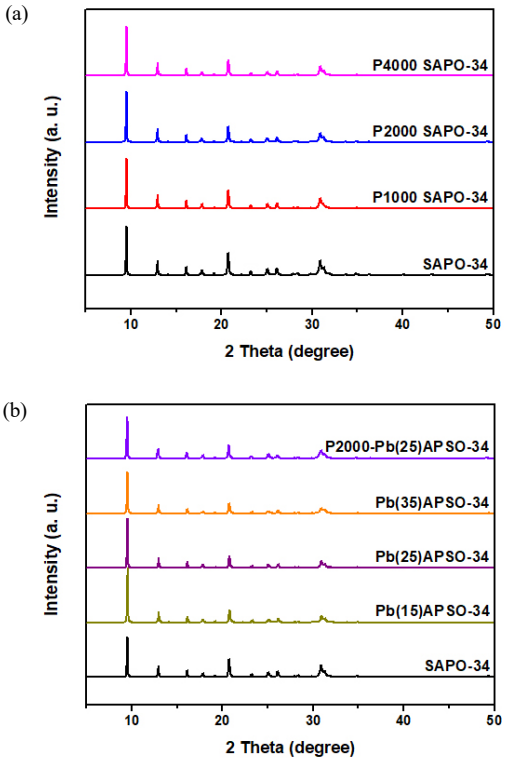

Figure 1. XRD patterns of the SAPO-34 and modified SAPO-34 catalysts.

Figure 2 shows SEM images of the prepared catalysts. The unmodified SAPO-34 crystals exhibited cubic shapes and smooth surfaces in the size range of 1~5 μm (Figure 2 (a)). The surface of the hierarchical SAPO-34 catalysts was rougher than that of the unmodified SAPO-34 catalyst. This result indicates that PEG, as a mesopore directing agent, was inserted into the crystal during the catalyst crystallization[18]. As the molecular weight of the added PEG increased, the size of the catalyst crystals decreased. This result indicates that PEG not only introduces intracrystallinity into the catalyst but also acts as a crystal growth inhibitor[27]. Spherical crystals were observed in the Pb(35)APSO-34 catalyst. Lu reported that agglomerated crystals with high Zr contents were observed in the ZrAlPO catalyst in which Zr was synthesized[28]. It is considered that unsubstituted Pb atoms in the catalyst framework combine with other atoms to form spherical crystals. In the P2000-Pb(25)SAPO-34 catalyst, spherical crystals were formed compared with the Pb(25)APSO-34 prepared by adding Pb in an equal molar ratio. This result suggests that the formation of spherical crystals was promoted around Pb, and these crystals were not substituted into the catalyst framework due to the added PEG.

Table 2 shows the textural properties of the SAPO-34 and modified SAPO-34 catalysts. The SAPO-34 catalyst prepared by PEG addition showed an increased mesopore volume and external surface area compared to that of the unmodified SAPO-34 catalyst. Sun et al. reported that mesopores were introduced when PEG was added during the preparation of the SAPO-34 catalyst[19]. In addition, this result is in good

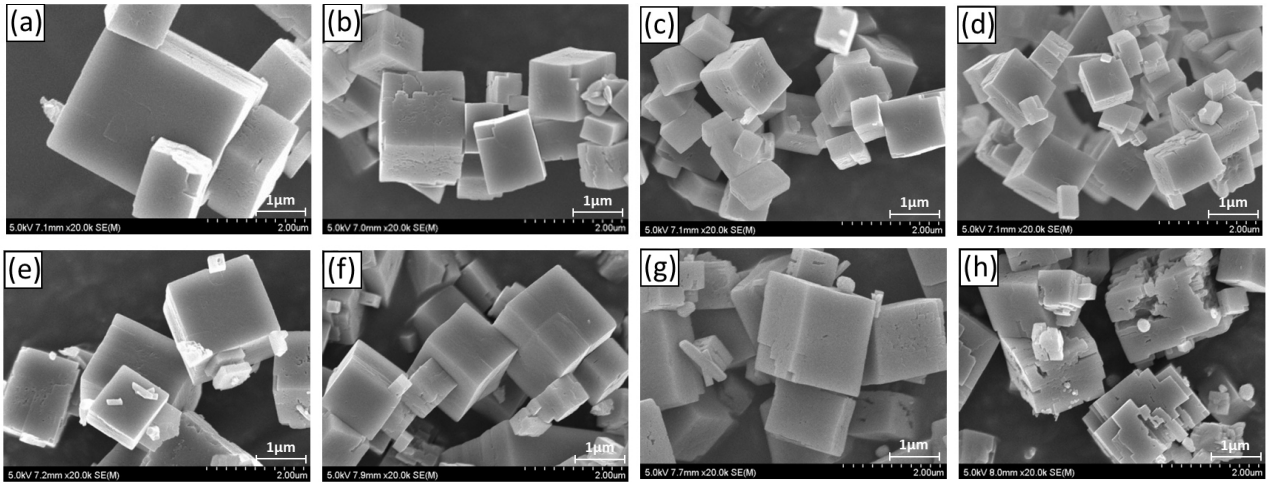

Figure 2. SEM images of the SAPO-34 and modified SAPO-34 catalysts: (a) SAPO-34, (b) P1000 SAPO-34, (c) P2000 SAPO-34, (d) P4000 SAPO-34, (e) Pb(15)APSO-34, (f) Pb(25)APSO-34, (g) Pb(35)APSO-34, and (h) P2000-Pb(25)APSO-34.

Table 2. Textural Properties of the SAPO-34 and Modified SAPO-34 Catalysts

Catalyst	S_{BET}[a] ($m^2 \cdot g^{-1}$)	S_{micro}[c] ($m^2 \cdot g^{-1}$)	S_{ext}[b] ($m^2 \cdot g^{-1}$)	V_{total}[a] ($cm^3 \cdot g^{-1}$)	V_{micro}[b] ($cm^3 \cdot g^{-1}$)	V_{meso}[c] ($cm^3 \cdot g^{-1}$)
SAPO-34	511	502	9	0.280	0.269	0.011
P1000 SAPO-34	513	500	13	0.295	0.259	0.036
P2000 SAPO-34	533	517	16	0.313	0.266	0.047
P4000 SAPO-34	526	508	18	0.319	0.265	0.054
Pb(15)APSO-34	528	516	12	0.282	0.267	0.015
Pb(25)APSO-34	536	523	13	0.287	0.269	0.018
Pb(35)APSO-34	523	512	11	0.277	0.266	0.011
P2000-Pb(25)APSO-34	525	510	15	0.282	0.254	0.028

[a] BET surface area and total pore volume were derived by applying the multi-point BET-model.
[b] External surface area and micropore volume determined by t-plot.
[c] $S_{micro} = S_{BET} - S_{ext}$, $V_{meso} = V_{total} - V_{micro}$.

agreement with the SEM image result showing a rough surface, in which PEG inserts in the catalyst crystals during the crystallization process. Therefore, it was confirmed that as a mesopore directing agent, PEG can successfully form a hierarchical structure. The BET surface area of the Pb(15)APSO-34 and Pb(25)APSO-34 catalysts increased compared with that of the unmodified SAPO-34 catalyst, while the BET surface area of the Pb(35)APSO-34 catalyst was reduced. This means that the formation of the CHA structure was promoted during the crystallization process by the addition of Pb, but as the Pb content increased, the formation of the CHA structure was hindered, thereby impairing the pore properties[29]. These results are consistent with the relative crystallinity mentioned above (Table 1). The P2000-Pb(25) APSO-34 catalyst showed an increased mesopore volume compared to that of the unmodified SAPO-34 catalyst and a small mesopore volume compared to that of the P2000 SAPO-34 catalyst. Varzaneh et al. reported that the hierarchical ZrAPSO-34 catalyst prepared by adding CNTs and Zr exhibited impaired pore properties due to a decrease in crystallinity, resulting in a reduced mesopore volume and BET surface area compared to that of the hierarchical SAPO-34 catalyst. This result is considered to involve the impairment of pore properties due to a decrease in crystallinity, which occurs after Pb is incorporated into the framework of the SAPO-34 catalyst[30].

The result of XPS analysis, which was performed to confirm the chemical bonding state of the prepared catalyst surface, is illustrated in Figure 3. A peak corresponding to the XPS spectrum of Si2p was observed in the range of approximately 100~105 eV (Figure 3 (a)). The intensity of the detected Si2p peak appeared in the following order: P2000-Pb(25)APSO-34 > SAPO-34 > Pb(25)APSO-34. The peak intensity of Si2p indicates the number of bound Si[31]. The Pb(25) APSO-34 catalyst showed a lower peak intensity than that of the unmodified SAPO-34 catalyst, indicating that Si was not substituted with P from the P-O-Pb frameworks[14]. The P2000-Pb(25)APSO-34 catalyst showed the highest peak intensity of Si2p. The added PEG is considered to promote the substitution of Si atoms into the catalyst framework. The Pb4f XPS spectra were observed at approximately 139.6 eV and 144.5 eV, indicating Pb4f7/2 and Pb4f5/2 peaks, respectively[32]. The positions of the detected Pb4f peaks correspond to the binding state of Pb^{2+}[33]. This result demonstrates that Pb of the

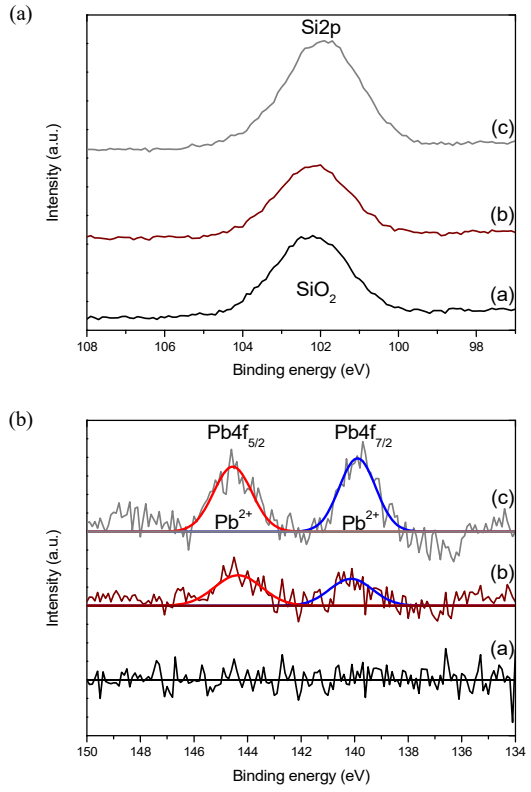

Figure 3. XPS Si2p and Pb4f spectra for SAPO-34 and modified SAPO-34 catalysts: (a) SAPO-34, (b) Pb(25)APSO-34, and (c) P2000-Pb(25)APSO-34.

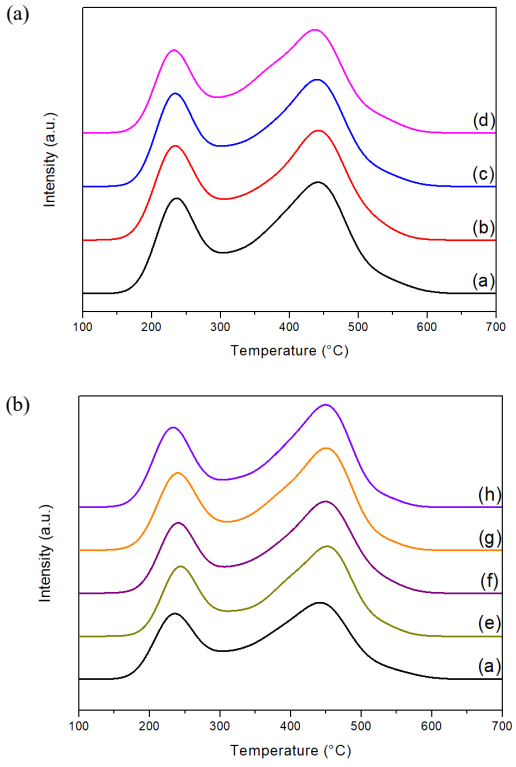

Figure 4. NH_3-TPD patterns of the SAPO-34 and modified SAPO-34 catalysts: (a) SAPO-34, (b) P1000 SAPO-34, (c) P2000 SAPO-34, (d) P4000 SAPO-34, (e) Pb(15)APSO-34, (f) Pb(25)APSO-34, (g) Pb(35) APSO-34, and (h) P2000-Pb(25)APSO-34.

divalent cation form (Pb^{2+}) was substituted with Al^{3+} of the catalyst framework to generate acid sites[34]. The peak intensity of the P2000-Pb(25)APSO-34 catalyst was increased in both the Pb4f7/2 and Pb4f5/2 peaks compared to that of the Pb(25)APSO-34 catalyst. This result indicated that the substitution of Pb into the catalyst framework was promoted by the added PEG and was consistent with the Si XPS results.

NH_3-TPD was carried out to analyze the acid strength and acid site concentration of the prepared catalysts. The NH_3-TPD profile and acidic properties are presented in Figure 4 and Table 3, respectively. Two NH_3 desorption peaks were observed in all catalysts. The desorption peaks at low (233~243 °C) and high (442~453 °C) temperatures are attributed to weak and strong acid sites, respectively[35]. The weak acid sites indicate T-OH (T: Si, P, Al) hydroxyl groups due to structural defects. The strong acid sites are Bronsted acid sites, in which Si-OH-Al bonds are created by the isomorphous substitution of Si^{4+} and P^{5+} in the P-O-Al frameworks[36]. The concentration of acid sites and acid strength of the hierarchical SAPO-34 catalyst decreased as the molecular weight of the added PEG increased. It has been reported that mesopore directing agents cause crystal defects in the catalyst, resulting in reduced Si contents[14,25]. Therefore, it is considered that the acidity of the hierarchical SAPO-34 catalyst decreased due to defects in the crystal structure, which were caused by the addition of PEG, and this result is in good agreement with the relative crystallinity results

Table 3. Calculated Acidity of the SAPO-34 and Modified SAPO-34 Catalysts

Catalyst	Acidity : NH_3 desorption amounts ($mmol \cdot g^{-1}$)		
	Weak (233~243 °C)	Strong (437~453 °C)	Total amount
SAPO-34	0.548	0.789	1.337
P1000 SAPO-34	0.534	0.776	1.310
P2000 SAPO-34	0.513	0.748	1.261
P4000 SAPO-34	0.460	0.744	1.204
Pb(15)APSO-34	0.565	0.806	1.371
Pb(25)APSO-34	0.616	0.828	1.444
Pb(35)APSO-34	0.627	0.953	1.580
P2000-Pb(25)APSO-34	0.665	0.918	1.583

in Table 1. The acidity of the PbAPSO-34 catalyst increased as the amount of added Pb increased. The arrangements of Si atoms were adjusted by substituting metal atoms into the frameworks of the SAPO-34 catalyst. Si islands are created by adjusting the atomic arrangement of Si [14]. This results in the formation of more acid sites on the SAPO-34 catalyst. Therefore, the increase in acidity of the PbAPSO-34 catalyst is due to the acid sites generated by Pb being incorporated into the catalyst frameworks[37]. The P2000-Pb(25)APSO-34 catalyst showed the highest concentration of acid sites. This was due

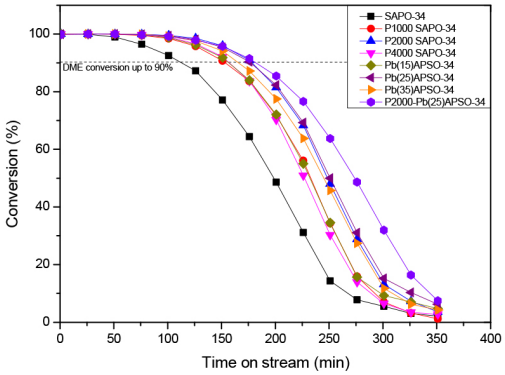

Figure 5. DME conversion of the SAPO-34 and modified SAPO-34 catalysts.

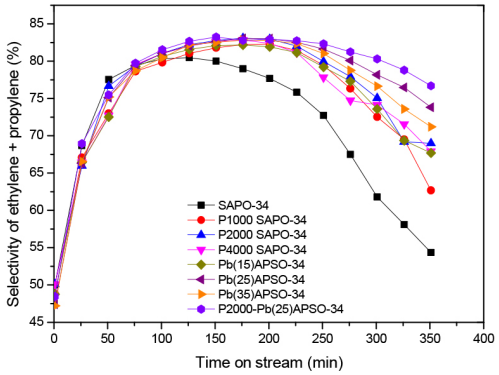

Figure 6. Selectivity of light olefins (ethylene + propylene) in DTO reaction over SAPO-34 and modified SAPO-34 catalysts.

to the increase in the number of incorporations for Si and Pb in the P2000-Pb(25)APSO-34 catalyst, as observed by XPS.

3.2. Catalytic performance in DTO reaction

The performance of the SAPO-34 and modified SAPO-34 catalysts was evaluated through the DTO reaction. The DME conversion for the prepared catalysts is shown in Figure 5. The catalytic lifetime was based on a DME conversion of over 90%. The unmodified SAPO-34 catalyst showed a DME conversion of 100% at the beginning of the reaction but was rapidly deactivated with the times on stream. These rapid deactivations of unmodified SAPO-34 catalyst were attributed to the blockage of active sites and limited mass transfer of reactants and products by coke deposition[38].

The hierarchical SAPO-34 catalysts exhibited an improved catalytic lifetime. In particular, the P2000 SAPO-34 catalyst showed the highest catalytic lifetime (178 min) among the PEG-modified SAPO-34 catalysts. Introducing PEG into the SAPO-34 catalysts resulted in the formation of mesopores and reduced acidity. It has been reported that the introduction of mesopores into catalyst crystals enhances the mass transfer of reactants and products[19]. In addition, the rapid DME conversion is inhibited by the reduced acidity of catalysts, so the production of reaction intermediates such as HMB is delayed. As a result, mild reaction conditions are induced in the SAPO-34 catalyst[15]. Therefore, the hierarchical SAPO-34 catalysts that involved delayed coke formation by improved mass transfer and reduced acidity exhibited an enhanced catalytic lifetime.

All of the PbAPSO-34 catalysts showed superior catalytic lifetimes compared to that of the unmodified SAPO-34 catalyst. The introduction of Pb into the catalyst frameworks enhanced the growth of CHA structures, resulting in an improved BET surface area. In addition, the acidity of the PbAPSO-34 catalyst was increased by the additional generation of acid sites and the variation in the arrangement of catalyst frameworks due to Pb incorporation. Although an increase in acidity improves reactivity, excessive acidity leads to the deactivation of catalysts due to rapid coke deposition[39]. Kim et al. reported that the performance of the MeAPSO-34 (Me = Fe^{2+}, Ni^{2+}, and Mn^{2+}) catalyst was improved by inducing mild reaction conditions due to a greater increase in the concentration of weak acid sites compared to the concentration of strong acid sites[14]. Therefore, it seems that the Pb(15)APSO-34 and Pb(25)APSO-34 catalysts, in which the concentration of weak acid sites increased more than that of strong acid sites, induced mild reaction conditions, resulting in superior catalytic lifetimes. However, in the Pb(35)APSO-34 catalyst, compared to the weak acid sites, the strong acid sites exhibited a greater increase in concentration. For this reason, it is considered that the Pb(35)APSO-34 catalyst exhibited a lower catalytic activity due to a rapid reaction of reactants. Consequently, the Pb(25)APSO-34 catalyst showed the longest catalytic lifetime (179 min) among the catalysts modified by Pb, and it was confirmed that the Pb/Al molar ratio of 0.0025 was the optimal addition condition.

The P2000-Pb(25)APSO-34 catalyst was prepared by simultaneously adding a PEG molecular weight of 2000 and a Pb/Al molar ratio of 0.0025, which were the optimal conditions among the PEG and Pb addition conditions, to the catalyst synthesis procedure. The P2000-Pb(25)APSO-34 catalyst exhibited the longest catalytic lifetime (183 min) among all catalysts and showed delayed deactivation at a DME conversion of less than 90%. However, the catalytic lifetime was not significantly improved compared to that of the P2000 SAPO-34 catalyst and Pb(25)APSO-34 catalyst that were prepared by adding PEG and Pb under the same conditions, respectively. This result is related to the increased concentration of acid sites in the NH_3-TPD results of the P2000-Pb(25)APSO-34 catalyst. The addition of PEG introduced mesopores to the SAPO-34 catalyst but promoted the substitution of Si and Pb into the catalyst frameworks, resulting in an increase in the concentration of acid sites. In particular, compared to the concentration of weak acid sites, that of the strong acid sites significantly increased. Excess strong acid sites promote the reaction of reactants, resulting in rapid coke deposition[37]. Therefore, in the P2000-Pb(25)APSO-34 catalyst, the mass transfer of reactants and products was improved by introducing mesopores, but coke deposition was promoted due to the relatively significant increase in concentration of strong acid sites.

The light olefin (ethylene, propylene) selectivity of the SAPO-34 catalyst and modified SAPO-34 catalysts is illustrated in Figure 6. At the beginning of the reaction, all catalysts exhibited a selectivity for light olefins of approximately 50%. Then, as the reaction proceeded,

the selectivity of light olefins increased over 80%. The SAPO-34 catalyst showed the best light olefin selectivity (approximately 80%), which was the lower compared to that of the modified catalyst. The selectivity of light olefins for hierarchical SAPO-34 and PbAPSO-34 catalysts modified with PEG and Pb increased by approximately 2-3% compared to that of the unmodified SAPO-34 catalyst. This was due to the improved mass transfer of reactants and products by the introduction of mesopores and the mild reaction conditions induced by the incorporation of Pb[40]. In the case of the P2000-Pb(50)APSO-34 catalyst, although mesopores were introduced into the catalyst crystals, the concentration of acid sites increased significantly. Thus, the selectivity of light olefins was not significantly enhanced compared to that of the P2000 SAPO-34 and Pb(25)APSO-34 catalysts.

4. Conclusions

In this study, SAPO-34 catalysts modified with PEG and Pb were prepared, and the effects of various PEG molecular weights and Pb/Al molar ratios on catalyst performance were investigated. PEG was introduced into the catalyst crystals, resulting in the formation of mesopores. In addition, as the molecular weight of the added PEG increased, the acidity of the modified SAPO-34 catalysts tended to decrease. The mesopores introduced into the SAPO-34 catalysts improved the mass transfer of reactants and products, and the reduced acidity induced a mild reaction. Thus, the SAPO-34 catalysts that contained hierarchical structures exhibited improved catalytic performance due to delayed coke formation. In particular, the P2000 SAPO-34(178 min) catalyst showed the longest catalytic lifetime, with an improvement of approximately 57% compared to that of the unmodified SAPO-34 catalyst (113 min). The Pb atoms were successfully substituted into the frameworks of the SAPO-34 catalyst. As the amount of added Pb increased, the acidity of the catalyst improved. In addition, the concentrations of weak acid sites, which induce a mild reaction, were increased compared with those of the strong acid sites. In particular, the Pb(25)APSO-34 catalyst showed the highest concentrations of weak acid sites. The BET surface area increased as the added Pb/Al molar ratio increased to 0.0025. Accordingly, the PbAPSO-34 catalyst resulted in improved catalytic performance. The P2000-Pb(25)APSO-34 catalyst exhibited the longest catalytic lifetime of 183 min and delayed deactivation among the synthesized catalysts. PEG played a role in mesopore-directing agents despite the coaddition of Pb. However, the substitution of Pb and Si into the frameworks of SAPO-34 catalysts was promoted by the addition of PEG, resulting in an increased concentration of acid sites. The mass transfers of reactants and products were enhanced by the introduction of mesopores. However, the higher concentration of strong acid sites compared to the weak acid sites accelerated the reaction of the reactants, resulting in encouraged coke deposition. Therefore, the performance of the P2000-Pb(25)APSO-34 catalyst was not significantly improved compared to that of the P2000 SAPO-34 catalyst and the Pb(25)APSO-34 catalyst that were prepared by adding PEG and Pb under the same conditions, respectively.

Acknowledgements

This work was supported by research fund of Chungnam National University.

References

1. M. A. B. Siddiqui, A. M. Aitani, M. R. Saeed, and S. Al-Khattaf, Enhancing the production of light olefins by catalytic cracking of FCC naphtha over mesoporous ZSM-5 catalyst, *Top. Catal.*, **53**, 1387-1393 (2010).
2. S. Ilias and A. Bhan, Mechanism of the catalytic conversion of methanol to hydrocarbons, *ACS Catal.*, **3**, 18-31 (2013).
3. U. Olsbye, S. Svelle, M. Bjørgen, P. Beato, T. V. W. Janssens, F. Joensen, S.Bordiga, and K. P. Lillerud, Conversion of methanol to hydrocarbons: how zeolite cavity and pore size controls product selectivity, *Angew. Chem. Int. Ed.*, **51**, 2-24 (2012).
4. C. Wang, X. Pan, and X. Bao, Direct production of light olefins from syngas over a carbon nanotube confined iron catalyst, *Chin. Sci. Bull.*, **55**, 1117-1119 (2010).
5. D. Xiang, Y. Qian, Y. Man, and S. Yang, Techno-economic analysis of the coal-to-olefins process in comparison with the oil-to-olefins process, *Appl. Energy*, **113**, 639-647 (2014).
6. Y. Liu, J. F. Chen, J. Bao, and Y. Zhang, Manganese-modified Fe_3O_4 microsphere catalyst with effective active phase of forming light olefins from syngas, *ACS Catal.*, **5**, 3905-3909 (2015).
7. G. Seo and B. G. Min, Mechanism of methanol conversion over zeolite and molecular sieve catalysts, *Korean Chem. Eng. Res.*, **44**, 329-339 (2006).
8. J. Lefevere, S. Mullens, V. Meynen, and J. V. Noyen, Structured catalysts for methanol-to-olefins conversion: A review, *Chem. Pap.*, **68**, 1143-1153 (2014).
9. T. Dogu and D. Varisli, Alcohols as alternatives to petroleum for environmentally clean fuels and petrochemicals, *Turk. J. Chem.*, **31**, 551-567 (2007).
10. S. G. Lee, H. S. Kim, Y. H. Kim, E. J. Kang, D. H. Lee, and C. S. Park, Dimethyl ether conversion to light olefins over the SAPO-34/ZrO_2 composite catalysts with high lifetime, *J. Ind. Eng. Chem.*, **20**, 61-67 (2014).
11. H. Huang, M. Yu, Q. Zhang, and C. Li, Mechanistic study on the effect of ZnO on methanol conversion over SAPO-34 zeolite, *Catal. Commun.*, **137**, 105932 (2020).
12. E. Aghaei, M. Haghighi, Z. Pazhohniya, and S. Aghamohammadi, One-pot hydrothermal synthesis of nanostructured ZrAPSO-34 powder: Effect of Zr-loading on physicochemical properties and catalytic performance in conversion of methanol to ethylene and propylene, *Micropor. Mesopor. Mater.*, **226**, 331-343 (2016).
13. D. Zhang, Y. Wei, L. Xu, F. Chang, Z. Liu, S. Meng, B. L. Su, and Z. Liu, MgAPSO-34 molecular sieves with various Mg stoichiometries: Synthesis, characterization and catalytic behavior in the direct transformation of chloromethane into light olefins, *Micropor. Mesopor. Mater.*, **116**, 684-692 (2008).
14. H. S. Kim, S. G. Lee, Y. H. Kim, D. H. Lee, J. B. Lee, and C. S. Park, Improvement of lifetime using transition metal-incorporated SAPO-34 catalysts in conversion of dimethyl ether to light olefins, *J. Nanomater.*, **2013**, 679758 (2013).
15. S. Zhang, Z. Wen, L. Yang, C. Duan, X. Lu, Y. Song, Q. Ge, and

Y. Fang, Controllable synthesis of hierarchical porous petal-shaped SAPO-34 zeolite with excellent DTO performance, *Micropor. Mesopor. Mater.*, **274**, 220-226 (2019).
16. M. Razavian and S. Fatemi, Fabrication of SAPO-34 with tuned mesopore structure, *Z. Anorg. Allg. Chem.*, **640**, 1855-1859 (2014).
17. F. Schmidt, S. Paasch, E. Brunner, and S. Kaskel, Carbon templated SAPO-34 with improved adsorption kinetics and catalytic performance in the MTO-reaction, *Micropor. Mesopor. Mater.*, **164**, 214-221 (2012).
18. E. J. Kang, D. H. Lee, H. S. Kim, K. H. Choi, C. S. Park, and Y. H. Kim, Conversion of DME to light olefins over mesoporous SAPO-34 catalyst prepared by carbon nanotube template, *Appl. Chem. Eng.*, **25**, 34-40 (2014).
19. Q. Sung, N. Wang, G. Guo, X. Chen, and J. Yu, Synthesis of tri-level hierarchical SAPO-34 zeolite with intracrystalline micro–meso–macroporosity showing superior MTO performance, *J. Mater. Chem. A*, **3**, 19783-19789 (2015).
20. Q. Sun, Z. Xie, and J. Yu, The state-of-the-art synthetic strategies for SAPO-34 zeolite catalysts in methanol-to-olefin conversion, *Natl. Sci. Rev.*, **5**, 542-558 (2018).
21. Y. Chai, L. Xie, Z. Yu, W. Dai, G. Wu, N. Guan, and L. Li, Lead-containing Beta zeolites as versatile Lewis acid catalysts for the aminolysis of epoxides, *Micropor. Mesopor. Mater.*, **264**, 230-239 (2018).
22. A. Güngör, R. Genç, and T. Özdemir, Facile synthesis of semiconducting nanosized 0D and 2D lead oxides using a modified co-precipitation method, *J. Turk. Chem. Soc. A: Chem.*, **4**, 1017-1030 (2017).
23. M. B. Brahim, S. Soukrata, H. B. Ammar, and Y. Samet, Study on anodic oxidation parameters for removal of pesticide imidacloprid on a modified tantalum surface by lead dioxide film, *Glob. Nest. J.*, **22**, 48-54 (2020).
24. K. Mirza, M. Ghadiri, M. Haghighi, and A. Afghan, Hydrothermal synthesize of modified Fe, Ag and K-SAPO-34 nanostructured catalysts used in methanol conversion to light olefins, *Micropor. Mesopor. Mater.*, **260**, 155-165 (2018).
25. A. Z. Varzaneh, J. Towfighi, and S. Sahebdelfar, Carbon nanotube templated synthesis of metal containing hierarchical SAPO-34 catalysts: Impact of the preparation method and metal avidities in the MTO reaction, *Micropor. Mesopor. Mater.*, **236**, 1-12 (2016).
26. X. Hu, L. Yuan, S. Cheng, J. Luo, H. Sun, S. Li, L. Li, and C. Wang, GeAPSO-34 molecular sieves: synthesis, characterization and methanol-to-olefins performance, *Catal. Commun.*, **123**, 38-43 (2019).
27. Y. Wang, Z. Wang, C. Sun, H. Chen, H. Li, and H. Li, Performance of methanol-to-olefins catalytic reactions by the addition of PEG in the synthesis of SAPO-34, *Trans. Tianjin Univ.*, **23**, 501-510 (2017).
28. J. M. Lü, K. T. Ranjit, P. Rungrojchaipan, and L. Kevan, Synthesis of mesoporous aluminophosphate (AlPO) and investigation of zirconium incorporation into mesoporous AlPOs, *J. Phys. Chem. B*, **109**, 9284-9293 (2005).
29. M. D. Rami, M. Taghizadeh, and H. Akhoundzadeh, Synthesis and characterization of nano-sized hierarchical porous AuSAPO-34 catalyst for MTO reaction: special insight on the influence of TX-100 as a cheap and green surfactant, *Micropor. Mesopor. Mater.*, **285**, 259-270 (2019).
30. A. Z. Varzaneh, J. Towfighi, and M. S. Moghaddam, Synthesis of zirconium modified hierarchical SAPO-34 catalysts using carbon nanotube template for conversion of methanol to light olefins, *Pet. Chem.*, **60**, 204-211 (2020).
31. M. H. Engelhard, D. R. Baer, A. H. Gomez, and P. M. A. Sherwood, Introductory guide to backgrounds in XPS spectra and their impact on determining peak intensities, *J. Vac. Sci. Technol. A*, **38**, 063203 (2020).
32. J. G. Dillard, M. H. Koppelman, D. L. Crowther, C. V. Schenck, J. W.Murray, and L. Balistrieri, X-ray photoelectron spectroscopic (XPS) studies on the chemical nature of metal ions adsorbed on clays and minerals. In: P. H. Tewari (ed.). *Adsorption from Aqueous Solutions*, 227-240, Springer, Boston, MA (1981)
33. M. Azuma, Y. Sakai, T. Nishikubo, M. Mizumaki, T. Watanuki, T. Mizokawa, K. Oka, H. Hojo, and M. Naka, Systematic charge distribution changes in Bi- and Pb-3d transition metal perovskites, *Dalton Trans.*, **47**, 1371-1377 (2018).
34. G. Ping, K. Zheng, Q. Fang, and G. Li, Composite nanostructure of manganese cluster and CHA-type silicoaluminaphosphates: enhanced catalytic performance in dimethylether to light olefins conversion, *Nanomaterials*, **11**, 24 (2021).
35. C. Sun, Y. Wang, Z. Wang, H. Chen, X. Wang, H. Li, L. Sun, C. Fan, C. Wang, and X. Zhang, Fabrication of hierarchical ZnSAPO-34 by alkali treatment with improved catalytic performance in the methanol-to-olefin reaction, *C. R. Chimie*, **21**, 61-70 (2018).
36. K. Song, Y. C. Yoon, C. S. Park, and Y. H. Kim, Effect of etching treatment of SAPO-34 catalyst on dimethyl ether to olefins reaction, *Appl. Chem. Eng.*, **32**, 20-27 (2021).
37. H. S. Kim, S. G. Lee, K. H. Choi, D. H. Lee, C. S. Park, and Y. H. Kim, Effects of Co/Al and Si/Al molar ratios on DTO (dimethyl ether to olefins) reaction over CoAPSO-34 catalyst, *Appl. Chem. Eng.*, **26**, 138-144 (2015).
38. D. Chen, K. Moljord, and A. Holmen, A methanol to olefins review: Diffusion, coke formation and deactivation on SAPO type catalysts, *Micropor. Mesopor. Mater.*, **164**, 239-250 (2012).
39. Q. Peng, G. Wang, Z. Wang, R. Jiang, D. Wang, J. Chen, and J. Huang, Tuning hydrocarbon pool intermediates by the acidity of SAPO-34 catalysts for improving methanol-to-olefins reaction, *ACS Sustain. Chem. Eng.*, **6**, 16867-16875 (2018).
40. S. Soltanali and J. T. Darian, Synthesis of mesoporous SAPO-34 catalysts in the presence of MWCNT, CNF, and GO as hard templates in MTO process, *Powder Technol.*, **355**, 127-134 (2019).

Authors

Kang Song; M.Sc., Graduate Student, Department of Chemical Engineering and Applied Chemistry, Chungnam National University, Daejeon 34134, Republic of Korea; thdrkd1203@naver.com
Jeong Hyeon Lim; M.Sc., Graduate Student, Department of Chemical Engineering and Applied Chemistry, Chungnam National University, Daejeon 34134, Republic of Korea; limjh0624@naver.com
Young Chan Yoon; M.Sc., Graduate Student, Department of Chemical Engineering and Applied Chemistry, Chungnam National University, Daejeon 34134, Republic of Korea; yyc7279@naver.com
Ju Sik Park; Ph.D., Senior Researcher, Korea Institute of Energy Research, Daejeon 34129, Republic of Korea; cspark@kier.re.kr
Young Ho Kim; Ph.D., Professor, Department of Chemical Engineering and Applied Chemistry, Chungnam National University, Daejeon 34134, Republic of Korea; yh_kim@cnu.ac.kr